5-10-2001

Spatial variability in the flow of a valley glacier: Deformation of a large array of boreholes

Joel T. Harper
University of Montana - Missoula, joel.harper@mso.umt.edu

Neil Humphrey
University of Wyoming

W. Tad Pfeffer
University of Colorado Boulder

Snehalata V. Huzurbazar
University of Wyoming

David B. Bahr
University of Colorado Boulder

See next page for additional authors

Recommended Citation

Harper, Joel T.; Humphrey, Neil; Pfeffer, W. Tad; Huzurbazar, Snehalata V.; Bahr, David B.; and Welch, Brian C., "Spatial variability in the flow of a valley glacier: Deformation of a large array of boreholes" (2001). *Geosciences Faculty Publications*. 26.
https://scholarworks.umt.edu/geosci_pubs/26

JOURNAL OF GEOPHYSICAL RESEARCH, VOL. 106, NO. B5, PAGES 8547-8562, MAY 10, 2001

Spatial variability in the flow of a valley glacier: Deformation of a large array of boreholes

Joel T. Harper,[1] Neil F. Humphrey,[2] W. Tad Pfeffer,[1] Snehalata V. Huzurbazar,[3] David B. Bahr,[1] and Brian C. Welch[2]

Abstract. Measurements of the deformation of a dense array of boreholes in Worthington Glacier, Alaska, show that the glacier moves with generally bed-parallel motion. Strain in the 200 m deep valley glacier is constant near the surface but follows a nonlinear vertical profile below a depth of about 120 m. By a depth of 180 m, the octahedral strain rate reaches 0.35 yr^{-1}. The three-dimensional velocity field shows spatial complexity with significant deviations from plane strain, despite relatively simple valley geometry in the vicinity of the 6×10^6 m^3 study volume. No evidence was found for time-varying deformation or movement along localized shear planes. Observations were made by repeatedly measuring the long-axis geometry of 31 closely spaced boreholes over a 70 day period, and three additional holes after 1 full year of deformation. The holes were spaced 15 to 30 m apart. Installation and measurement of such a large number of boreholes required the development of a semiautomated hot water drilling system that creates straight and vertical boreholes with uniform walls. The equipment and procedures enables borehole profiles to be measured without the use of hole casing. Inclinometry measurements collected in the holes were processed, analyzed for error, and visualized as a fully three-dimensional data set. The new methods offer unique insight into small-scale spatial and temporal variations in the pattern of flow in a valley glacier.

1. Introduction

Gravity is the constant force driving all glacier motion, yet observations suggest the processes that resist that force and thereby control glacier flow are not uniform in time or space. Temporal variations in glacier movement are well documented: numerous studies have demonstrated that motion can undergo strong diurnal and seasonal variations and that transient and localized velocity anomalies are not uncommon [e.g., *Meier*, 1960; *Brecher*, 1969; *Brzozowski and Hooke*, 1981; *Jacobel*, 1982; *Harrison et al.*, 1986; *Iken and Bindschadler*, 1986; *Krimmel and Vaughn*, 1987; *Meier et al.*, 1994]. Spatial variations in valley glacier movement has also been addressed by multiple studies [e.g., *Meier*, 1960; *Shreve and Sharp*, 1970; *Raymond*, 1971b; *Hooke et al.*, 1987, 1992; *Harbor et al.*, 1997], although most have focused primarily on depth variations in deformation, and flow patterns occurring over a length scale similar to or greater than the ice thickness. A notable exception is *Raymond's* [1971b] well-known study of Athabasca Glacier, Canada, which yielded two cross-valley profiles of the glacier's internal flow field. His results suggest smoothly varying velocity contours and flow paths approximately parallel with the valley geometry. However, one profile was constructed using data from just five boreholes and the other from three holes, all of which were spaced half the maximum ice depth apart. In contrast, *Harbor et al.*'s [1997] observations in closely spaced boreholes located within a partial cross section of Haut Glacier d'Arolla, Switzerland, suggest large variations in flow at a length scale much less than the ice depth. Thus the flow field in many valley glaciers might be significantly more complex than suggested by the measurements on Athabasca Glacier, but the three-dimensional complexity of the "short-wavelength" (i.e., less than the ice thickness) flow field has never before been documented.

Short-wavelength variations in the internal flow field may be particularly important in valley glaciers, where the width is typically less than 10 times the ice depth and longitudinal changes in slope and width are considerable. This geometry may lead to complex spatial variability due to the influence of the valley walls and longitudinal topography throughout the flow field. In addition, the characteristics of the ice, such as crystal size, bubble content, temperature and strain history, may change over short distances leading to further spatial differences in the deformation rate of the ice. While these factors may promote complicated structure in the flow field over short distances (i.e., fractions of an ice depth), the viscous rheology of the ice will tend to dampen short-wavelength variability.

[1]Institute of Arctic and Alpine Research, University of Colorado, Boulder, Colorado.
[2]Department of Geology and Geophysics, University of Wyoming, Laramie, Wyoming.
[3]Department of Statistics, University of Wyoming, Laramie, Wyoming.

Paper number 2000JB900440.
0148-0227/01/2000JB900440$09.00

This paper presents an observational data set that describes deformation in a valley glacier at a resolution that is similar in three dimensions, and much less (<10%) than the ice depth. Measurement of a fluid's three-dimensional flow field is nontrivial: consideration must be made to space/time averaging of measurements, and technological barriers, some specific to glaciers, are encountered. We first describe techniques for data collection and processing developed for the assembly and investigation of this data set. We offer analysis and discussion of the problems and limitations of three-dimensional deformation measurements in glaciers. Finally, we present the results of our measurement program conducted on Worthington Glacier, Alaska, revealing the three-dimensional pattern of flow within a large bulk sample of a temperate valley glacier.

2. Data Collection

2.1. Background

The most practical and efficient method for observing the internal flow field of a glacier is to measure the deformation of a borehole extending through its depth. The axial curvature of the borehole is tracked over time as it deforms with the moving ice, a procedure referred to as borehole inclinometry [*Raymond*, 1971a]. As the borehole is displaced along the valley with the flow field, a borehole deformation experiment measures the average flow field between the two positions at which the hole's curvature was determined.

Boreholes can be cased or, if drilled appropriately, holes can be left uncased. *Hooke et al.* [1987, 1992] used thin-walled aluminum casing in boreholes drilled into Storglaciären, Sweden. The casing was aligned in the hole so that a track in the casing wall maintained a constant azimuth at the time of installation. Therefore tilt alone was sufficient to determine the full curvature of the borehole (a far simpler measurement than azimuth). The casing gives the borehole a constant diameter and smooth walls so that inclinometry measurements are not influenced by local irregularities in the holes. A disadvantage of this method is that there can be differential movement between the casing and the borehole wall if the outside diameter of the casing does not perfectly match the diameter of the borehole. Maintaining a snug fit over a long period is difficult due the effects of deformation and pressure melting. The alternative is to leave the holes uncased. This, however, requires that azimuth be measured and introduces the possibility that tilt measurements may be corrupted by play of the inclinometer within irregular borehole walls.

Maintenance of boreholes against freezing and creep closure is necessary when inclinometry measurements are made over long time intervals. The life span of a borehole depends on the thermal structure of the glacier, the depth of the borehole, and the water level and circulation in the hole. Even in a temperate glacier during summer, freezing may occur at the surface due to lasting effects of the winter cold wave, and at depth due to upward movement of both ice and water at the pressure melting point [e.g., *Harrison*, 1972; *Alley et al.*, 1999]. Some boreholes in temperate glaciers may close in as little as 2 weeks; others may persist for several months. A method for maintaining boreholes for longer periods is to mark the position of the borehole with a strand of wire running along the length of the borehole. The borehole is allowed to freeze or deform closed and is then redrilled at a later time using a wire-following drill. This enables the curvature of borehole to be remeasured over a protracted time interval (i.e., one or more years). Questions remain, although, as to whether the wire regelates through the ice and eventually no longer represents the path of the original borehole.

2.2. This Study

Our field program had two primary data collection goals. The first was to measure the fully three-dimensional velocity field in a reach of glacier at a length scale of approximately 10% of the ice thickness. This was achieved through inclinometry in a 200 m deep glacier of an array of 31 closely spaced (20 ×30 m) boreholes as they were displaced 10-15 m in horizontal space. This displacement required a time interval of 60-70 days. The second objective was to measure the flow field in the same reach averaged over 1 year to be used for comparison. This was accomplished by inclinometry of three boreholes spaced 15×15 m after 1 year of deformation and a displacement equal to about one third of the ice depth.

2.2.1. Study reach. Field research was conducted on Worthington Glacier, a temperate valley glacier in the Chugach Mountains of Alaska (Figure 1). Worthington Glacier was chosen for its relatively uncomplicated geometry, active motion, and logistical simplicity. The study reach was just below the equilibrium line altitude of the 8 km long east-west running valley glacier and occupied a low-angle bench located between two icefalls. The icefalls are heavily fractured with deep and wide crevasses, multiple fracture directions, and numerous seracs, while the bench has long, narrow, and arcuate crevasses spaced 3-10 m apart. The average surface slope is ~10° along the entire glacier length, 2° to 3° in the study reach, and 20° to 25° through the icefalls. The reach has a volume of 6.2×10^6 m^3 and extends 230 m along-flow, 150 m across-flow, and is about 200 m in depth (Figure 2).

The reach has been the subject of several glaciological investigations. Boreholes drilled to the bed and ice-penetrating radar measurements were used to construct a map of the bed, which indicates that the ice thickness ranges from 185 to 210 m [*Welch et al.*, 1998]. Detailed observations of subsurface ice within the region made by analysis of borehole video images indicate that englacial structures such as voids

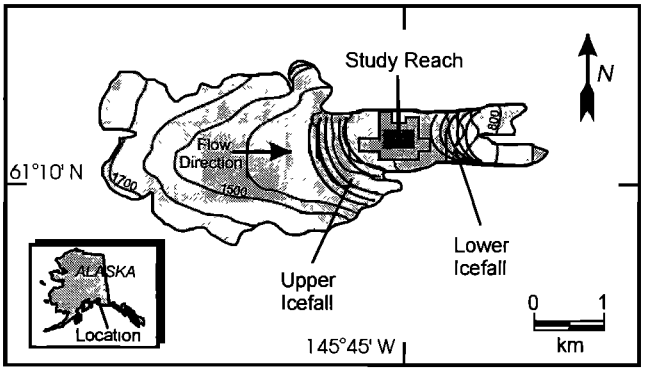

Figure 1. Map showing Worthington Glacier and the location of the study reach. Total length of the glacier is about 8 km and the surface slope averages 10 degrees.

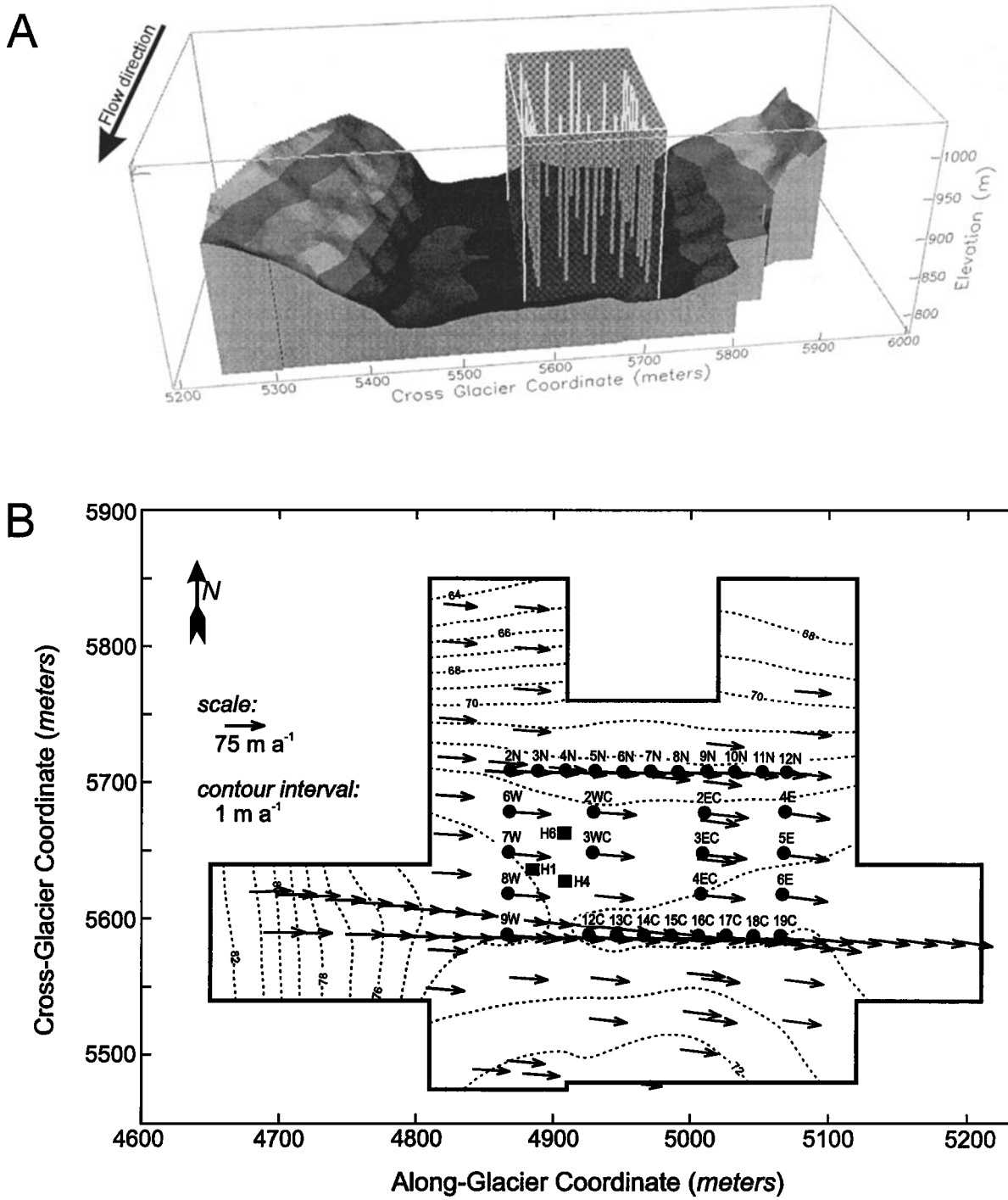

Figure 2. Maps of the study reach. (a) Perspective view looking up-glacier showing the location of 31 boreholes and the bed of the glacier as determined from radio-echo sounding measurements. Elevation ranges of the bed surface are displayed at 25 m intervals by grayscale. Box is region for which the three-dimensional velocity field was computed; vertical lines show boreholes. (b) Map view of study reach showing surface velocity vectors measured at 110 stakes (arrows), velocity contours (dashed lines), initial position of 31 boreholes used to construct three-dimensional flow field (solid circles), and 1997 position of boreholes used to measure deformation over 1 year (solid squares). Orientation of the reach with respect to the glacier is shown in Figure 1.

and clear ice layers make up a maximum of 3% of the ice mass [*Harper and Humphrey*, 1995]. Surface velocities in the reach have been observed to undergo strong diurnal and seasonal variations [*Harper et al.*, 1996]. Other work on this study reach has addressed the patterns of crevasses as they relate to the surface strain field [*Harper et al., 1998a*], time/space variations in the subglacial hydrology [*Stone et al.*, 1994], in situ stress measurements in ice [*Pfeffer et al.*, 1998, 2000], and long-term changes in the surface profile of the glacier [*Echelmeyer et al.*, 1996; *Sapiano et al.*, 1998].

2.2.2. Drilling. The logistics associated with drilling, maintaining, and measuring the large number of boreholes used in this project dictated that the drilling time for any one hole must be of the order of a few hours so that the entire array of holes could be established in a period of 1 to 2 weeks. Furthermore, with 31 boreholes totaling over 5.5 km in length, installing casing in the holes was not practical. Drilling multiple boreholes for uncased inclinometry, however, places stringent requirements on the drilling program. The holes need to be a specific diameter, in this case about 10 cm, and must have smooth walls. Straight and vertical boreholes are needed in order to avoid errors resulting from assumptions made during processing (described in section 3.4). To meet these objectives, new instrumentation and procedures for drilling and inclinometry were developed and implemented.

The boreholes were drilled by hot water methods [*Taylor, 1984*; *Engelhardt et al.*, 1990; *Humphrey and Echelmeyer*, 1990] using a system specifically designed to drill holes for uncased inclinometry. Straight and vertical holes with smooth walls and constant diameter were created by lowering a heavy (40 kg) drill stem by an electromechanical in-line drive. A load cell on the drill tower monitored the hanging weight of the drill stem to better than 1% precision giving constant input to a computer control of drilling speed. The hole diameter was restricted to 10 cm by the 200 cm long drill stem which had a tapered cross section along its length, from 3.4 to 1.4 cm. The unusually long and narrow stem caused turbulent mixing not just ahead of the drill tip but also within up-welling water along side the drill stem. The thermal decay length of the up-welling water was on the order of meters [*Humphrey and Echelmeyer*, 1990], and hence the long and narrow end of the drill stem gave turbulent eddies space to grow as they moved up the hole.

Following drilling, the boreholes were inspected for smoothness and diameter using a borehole video camera [*Harper and Humphrey*, 1995] and a digital-recording caliper lowered though the holes. These measurements revealed that the drilling system produced overly wide holes until the drill stem and high-pressure jet was submerged several meters within the borehole water column. Consequently, inclinometry data could not be collected in the top 5 to 8 m of the boreholes.

Boreholes were stopped about 10 m short of the bed. This was done to prevent circulation of borehole water arising from connection with the basal hydrologic system. Circulation advects water up or down the slight temperature gradient imposed by the Clausius-Clapeyron pressure-temperature relationship, leading to either thermal erosion or refreezing of the boreholes over time. Furthermore, with the holes nearly full of water, they were less likely to creep closed near the bottom. Two negative impacts of this decision were a lack of data in the immediate vicinity of the bed, and a tendency for some holes to freeze at the surface (holes drilled to the bed drain several tens of meters and hence do not contain water near the surface).

Refreezing of the boreholes was a problem that needed to be addressed after the boreholes were about 20-30 days old. Freezing occurred both near the surface and at depth and affected about a third of the boreholes with an apparent random distribution. Holes were maintained against freezing by redrilling with a specially designed reamer that focuses melting energy to only the parts of the borehole with a decreased diameter. After reaming, holes were reinspected with the video camera to assure that the hole geometry was not grossly altered by the reaming process.

2.2.3. Inclinometry. Borehole profiles were measured using a downhole digital inclinometer manufactured by Slope Indicator Canada Ltd. (Vancouver, British Columbia, Canada). The instrument determines inclination with two orthogonally mounted tilt meters and azimuth with a fluxgate magnetometer. These are mounted in a nonmagnetic stainless steel tube approximately 1.5 m in length. The tube remains centered in the hole at all times by flexible nonmagnetic centering springs. The instrument therefore averages its readings over a 1.5 m length of the borehole. Data are sent from the inclinometer to a laptop computer at the surface through a serial cable. Inclinometry measurements were made at 2 m intervals, and the boreholes were logged at least twice, once while lowering the instrument down the holes and once while raising it up. Raw measurements of tilt and azimuth were processed to produce the three-dimensional map of the borehole by software supplied with the inclinometer. The instrument and processing algorithm are described in detail by *Blake and Clarke* [1992].

Approximately 250 borehole profiles (up and down combined) were recorded with each of the 31 boreholes measured a minimum of four separate times during a 70 day period (Table 1). The holes were measured over 1 to 2 day intervals and each measurement group is classified as a "round." These measurements are categorized into inclinometry rounds 1-4 representing the first through fourth times the holes were measured. The data used for analysis are displacements between rounds 1-3 and rounds 1-4. These represent approximately 30 and 60 days of deformation, respectively. The tops of the boreholes and the larger array of surface stakes were surveyed 5 times during the same 70 day period.

The three boreholes used for measurements of year-long deformation were drilled during June of 1997. Each hole was fitted with a wire running along its entire length. The holes were then redrilled the following year using a specially designed wire-following drill tip. The redrilled holes were inclinometered, and their tops were surveyed in late June 1998. These measurements represent 372-374 days of deformation.

3. Data Processing

3.1. Borehole Maps

We define a right-handed local coordinate system for the glacier as x, y, z representing the along-glacier (horizontal and positive in the easterly direction of flow), cross-glacier (horizontal and positive north), and vertical (positive upward) directions, respectively. As our inclinometer determines only the deviation of points along a borehole relative to the top of the hole, several steps were followed in transforming the deviations into three-dimensional maps of the boreholes with coordinates of the local system (Figure 3).

1. Each hole was measured at least twice during each round of inclinometry. Measurements were averaged to form one profile representing the map for each round.

2. Surface ablation shortened the holes over the time. This effect was removed by adding the ablated ice elements back to the length of the borehole in data reduction, so that the

Table 1. Borehole Drilling and Inclinometry Dates, Julian Day 1994

Borehole	Drill	Round	Round	Round	Round	Δt^a			
	Day	1	2	3	4	Round 1	Round 2	Round 3	Round 4
6W	146	156	176			10	30		
7W	146	156	176	189		10	30	43	
8W	147	156	172	189	217	9	25	42	70
9W	148	161	176	189	217	13	28	41	69
2WC	148	156	180	187		8	32	39	
3WC	150	156	172	187	217	6	22	37	67
2EC	150	157	174	187	217	7	24	37	67
3EC	154	157	173	187	217	3	19	33	63
4EC	155	157	173	187	217	2	18	32	62
4E	155	160		190	217	5		35	62
5E	159	160	180	191	217	1	21	32	58
6E	158		180	189	216	0	22	31	58
12C	156	158	176	187	216	2	20	31	60
13C	156	157	176	187	216	1	20	31	60
14C	156	157	174	191	216	1	18	35	60
15C	155	157	174	191	216	2	19	36	61
16C	155	157	173	191	216	2	18	36	61
17C	157	158	170	189	216	1	13	32	59
18C	157	158	173	189	216	1	16	32	59
19C	157	158	180	189	216	1	23	32	59
3N	151	156	176	189		5	25	38	
4N	151	156		189		5		38	
5N	151	156	178	189	217	5	27	38	66
6N	154	156	178	187	217	2	24	33	63
7N	154	157	178	187		3	24	33	
8N	154	157	180	187		3	26	33	
9N	154	157	180	187	217	3	26	33	63
10N	160	160	180	189	217	0	20	29	57
11N	160	160		190,191		0		30, 31	
12N	159	160		190	217	1		31	58
97H1	166[b]		180[c]						
97H6	173[b]		180[c]						
97H4			180[c]						

[a] Number of days between drilling and inclinometry round.
[b] Julian day, 1997.
[c] Julian day, 1998.

length of the boreholes remained unchanged over the study period. Detailed measurements of surface ablation at the tops of the boreholes were required for this correction.

3. The top 20 m of each hole was set to zero displacement (a perfectly straight hole). Near-surface data were untrustworthy because the hole diameter of the upper portions of the boreholes was often wide and the inclinometer swung freely (giving invalid readings). Measurable tilt of the boreholes is not expected in the top 20 m since the surface parallel shear stress vanishes at the free surface.

4. Inclinometry data were transformed into a local coordinate system. The transformation required a rotation (from magnetic north to the local-coordinate y axis) and a horizontal translation of coordinates. As surveys were always made within a few days of the inclinometry measurements, but not necessarily at the exact moment, a linear interpolation between surveys of the top of each borehole was used to locate the top of the holes at the time of inclinometry. This step is essentially one of "hanging" the inclinometry data from the surface velocity field. Consequently, an error in locating a hole top would be propagated along the entire length of the hole. The survey procedures and analysis of error are described in detail by *Harper et al.* [1996].

3.2. Velocities

Measurement of the change in curvature of a borehole over time gives the shear strain in a plane normal to the trace of the hole but does not directly yield information about flow in the direction coaxial to the hole. Knowledge of the flow in the vertical direction enables the displacement of points along the hole to be tracked in three-dimensional space. This information is necessary to calculate both the vertical and horizontal velocity fields. Several attempts at measuring the surface-perpendicular strain rate have been made [e.g., *Harrison*, 1975; *Paterson*, 1976]; however, methods are time consuming and yield results with high measurement error. Only one such measurement was made here [*Harper*, 1997].

Instead of directly measuring vertical displacements, the surface perpendicular velocities were calculated from the

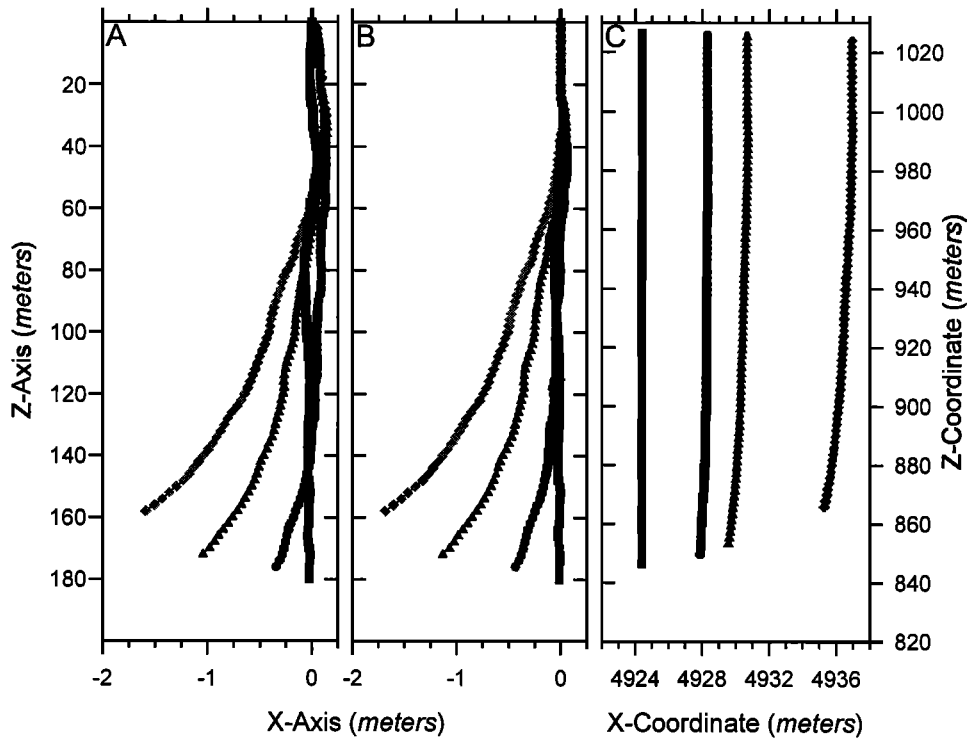

Figure 3. Procedure for processing of inclinometry data exemplified by borehole 5N. In all panels: squares, round 1; circles, round 2; triangles, round 3; diamonds, round 4. M (a) Pairs of up and down borehole maps were averaged to produce single profiles for each of the four rounds of inclinometry. (b) The upper 25 m of the profiles were set to zero offset due to inaccurate measurements caused by wide and irregular holes near the surface. (c) Hole maps were transformed into a local coordinate system to represent true displacements.

horizontal displacements within the array of adjacent boreholes using a method devised by *Raymond* [1971a]. The method assumes that ice in the region between the boreholes is incompressible and iteratively integrates the continuity condition over the region between the boreholes. Three orthogonal components of velocity are determined for a three-dimensional array of points, based on the criteria that the velocity gradients conserve volume within the array. The calculations require knowledge of the velocity gradients near the boreholes, which in this case were represented by interpolation functions fit to a combination of surface and borehole measurements. *Raymond*'s [1971a] iterative velocity calculation scheme was coded into a computer algorithm. Velocity values were computed at 2 m vertical intervals along lines projected vertically downward at the location of the initial borehole tops.

3.3. Interpolation

Velocities at the surface and along the boreholes were interpolated to an orthogonal grid, giving the three-dimensional velocity structure for a block of ice. Computations were done with velocity profiles produced from displacements between inclinometry Rounds 1-3, the only interval with significant deformation measured in a large number of holes. The interpolation used algorithms included in the EarthVision (Dynamic Graphics Inc., Alameda, California) software package, which are designed for interpolation of borehole data in the oil and gas industries. The procedure uses an iterative scheme to fit a cubic spline function with a minimum of curvature [*Briggs*, 1974]. The interpolated region was defined as a block with four planar sides and irregular top and bottom surfaces. The top of the block is defined by the surface of the glacier, while the bottom surface is parallel to the surface topography at a depth of 180 m. The 180 m cutoff represents the minimum length of the boreholes; not the actual bed surface. The total volume of the block is approximately 6.2×10^6 m^3.

3.4. Errors and Assumptions

3.4.1. Measurements. The borehole maps have errors that are associated with positioning the inclinometer at points in the borehole and errors related to measuring and computing the map. The inclinometer was located at discrete measurement points by visually aligning 2 m marks on the instrument cable with the top of the borehole. Alignment was done with an accuracy of 2-3 cm. The cable had a low-stretch kevlar core and the boreholes were mostly water filled, thus elongation of the cable as it was lowered into the hole was not significant. Since the instrument averaged measurements over a 1.5 m section of the borehole, the positioning error is assumed to have had no influence on results.

A combined error in the maps resulted from measurements of tilt and azimuth, and the subsequent computation of coordinate positions along the hole. The individual and combined effects of these errors have been investigated for a prototype of our instrument with both field and laboratory

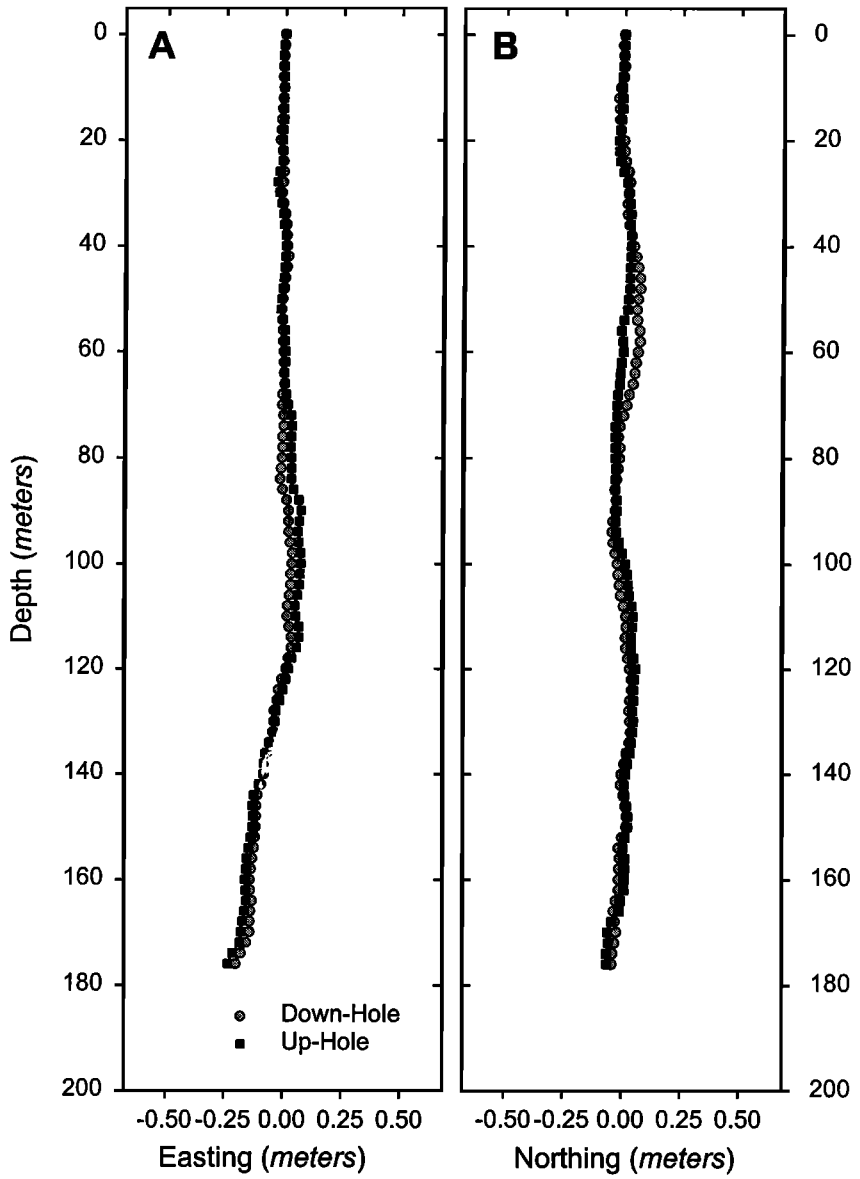

Figure 4. Measured trajectories of borehole 12C 6 days after it was drilled. Two trajectories are measured for each hole: one while lowering the inclinometer down the hole and one while raising it up. Horizontal exaggeration is 150 times.

testing by *Blake and Clarke* [1992]. Combined errors were found to be greatest in the azimuthal sense, mainly due to magnetometer performance. Errors in the coordinates of points along the hole increase away from the datum (top of the borehole) since each point is calculated as a departure from the next point closer to the datum. In addition, *Blake and Clarke* [1992] show through Monte Carlo simulations that the computational procedure tends to underestimate a hole's curvature.

We performed further analysis of the errors in our inclinometry data in order to describe confidence regions for our measurements. Here we use the term "error" to include instrument error as well as random error because the two are inseparable. We utilize the fact that we have at least two repeated measurements of each hole's profile (Figure 4). If each borehole were treated alone, the derived error estimate from simple consideration of the standard error in either the approximately along-glacier (x) direction or approximately cross-glacier (y) direction tends to be quite large and unreliable. In addition, the measurements in the x and y directions are correlated. Fortunately, the confidence regions can be improved through recognition of the fact that additional information about errors can be found by considering the structure of the errors in repeated inclinometry measurements, even though they are not of the same point. This strategy essentially pools whatever error information we have and thus maximizes our knowledge of the data. We restrict this analysis to inclinometry rounds 1, 2, and 3, where we have sufficient data.

We begin by assuming that error in depth (z) direction is minimal, so to estimate (x, y) coordinates of a point along the map for the i^{th} borehole in the j^{th} inclinometry round, at a fixed depth z, we use the average of the two sets of measurements (up and down), namely, (x_{ij}, y_{ij}). The behavior of the

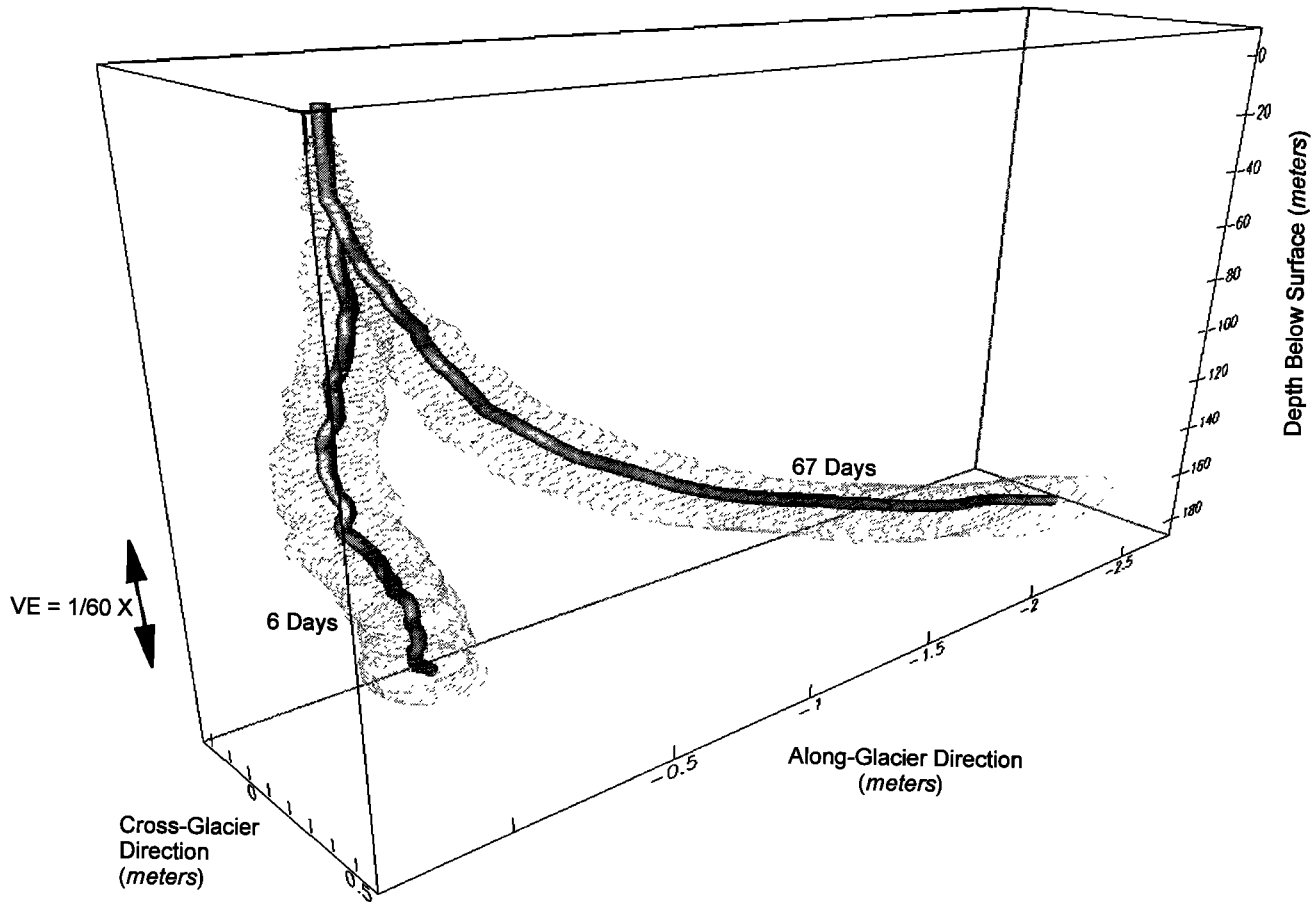

Figure 5. Perspective view of borehole 3WC 6 days and 67 days after it was drilled. Ellipses, computed at 2 m intervals, show 95% confidence regions for the measured trajectories. Vertical compression is 60 times.

errors in this average consists of the variation in the x direction (variance of x), and in the y direction (variance of y) as well as error variation common to both x and y (covariance of x and y). These components are found in the 2×2 covariance matrix for the (x, y) data at a fixed depth. For each borehole individually, estimation of this covariance matrix cannot be carried out since there are only two observations available; instead, we pool information at fixed depths from all the holes. The covariance matrix of the difference of the two observations divided by 2 is the same as that for the average of the two observations. The difference estimates are zero, and data on these weighted differenced observations (D), $\{(x_{ijD}, y_{ijD}), i = 1, \ldots, n\}$, are available from up to n = 31 holes. The estimate of the covariance matrix is

$$\frac{1}{n-1}\begin{bmatrix} \sum_{i=1}^{n}(x_{ijD}-\bar{x}_{jD})^2 & \sum_{i=1}^{n}(x_{ijD}-\bar{x}_{jD})(y_{ijD}-\bar{y}_{jD}) \\ \sum_{i=1}^{n}(x_{ijD}-\bar{x}_{jD})(y_{ijD}-\bar{y}_{jD}) & \sum_{i=1}^{n}(y_{ijD}-\bar{y}_{jD})^2 \end{bmatrix} = S_D , \quad (1)$$

where

$$\bar{x}_{jD} = \left(\frac{1}{n}\right)\sum_{i=1}^{n} x_{ijD}$$

and similarly for y_{jD}. Note that x_{jD} and y_{jD} are the averages, across the holes, of the difference between the up and down maps at a fixed depth. The diagonal terms are estimates of the variances in the x and y direction, respectively, and the off-diagonal term estimates the covariance of x and y. Using standard bivariate normal theory [e.g. *Johnson and Wichern*, 1988], a (1-α)100% confidence region for the (x, y) coordinates of the true map, μ,

$$\mu_{ij} = (\mu_{xij}, \mu_{yij})^T$$

is the region such that

$$m\begin{bmatrix}\bar{x}_{ij}-\mu_{xij}\\ \bar{y}_{ij}-\mu_{yij}\end{bmatrix} S_D^{-1} \begin{bmatrix}\bar{x}_{ij}-\mu_{xij}\\ \bar{y}_{ij}-\mu_{yij}\end{bmatrix} \le \frac{(n-1)p}{(n-p)} F_{p,n-p}(\alpha) \quad (2)$$

is the number of observations used to calculate the average (m = 2), n is the number of holes at the j^{th} level, p = 2 for the dimension of (x, y) and $F_{p,n-p}(\alpha)$ is the value from the F distribution with degrees of freedom p and n-p, so that the right tail probability is α. The shape of the region specified by (2) is an ellipse which is centered at the final map, $(x_{ij}, y_{ij})^T$. The orientations and lengths of the major and minor axes are given as follows. The covariance matrix S_D is

nonsingular and positive definite, so that its singular value decomposition yields (λ_1, $\mathbf{e}_1$) and (λ_2, $\mathbf{e}_2$), the two eigenvalue-eigenvector pairs, where $\lambda_1 > \lambda_2$. The eigenvector $\mathbf{e}_1$ gives the orientation of the major axis which has half-length

$$\sqrt{\lambda_1}\sqrt{\frac{(n-1)p}{m(n-p)}F_{p,n-p}(\alpha)} \quad . \tag{3}$$

Similarly, for the minor axis we have $\mathbf{e}_2$ replacing $\mathbf{e}_1$ and λ_2 replacing λ_1.

The size of the error ellipses gradually increases with depth due to the accumulation of errors away from the surface. An example borehole with error ellipses constructed at the 95% level is shown in Figure 5. Magnitudes of the axes of the error ellipse reach +/- 0.15 and 0.36 m at the bottom of the holes for the round 3 inclinometry. The long axis is generally aligned in the along-glacier direction, the direction of maximum deformation, and the minor axis of the error ellipse runs approximately cross glacier.

3.4.2. Calculations. Errors in calculating the velocities at points along the borehole trajectories stem from the implementation of *Raymond*'s [1971a] iterative velocity calculation scheme. We identify three such sources of potential error: (1) Interpolation functions are fit to velocity data so that both numerical differentiations and integrations can be made. We make the fundamental assumption that displacement data vary smoothly and fit with simple low-order polynomials. This assumption is supported by our observations of borehole displacements discussed in the following section, (2) Horizontal gradients in vertical velocity are assumed to be negligible over a length scale that is comparable to the horizontal offset between the top and bottom of the boreholes (in the case of round 1-3 data, about 2-4 m). The latter assumption is made so that the analysis can be simplified by calculating velocities along vertical lines falling straight below the tops of the holes, rather than for each of the points along the irregular borehole profiles. This is a reasonable assumption where surface slope gradients are small, as they were across the entire study reach, (3) Mass conservation is assumed. Consequently, volume changes caused by motion along crevasses at the surface are not accounted for. However, because crevasses are relatively small and widely spaced, and were both opening and closing within the reach [*Harper et al.*, 1998a], we believe that this assumption has a negligible impact on results.

The overall performance of the velocity calculation scheme was tested with a synthetic data set. Borehole displacements within a synthetic velocity field (satisfying continuity) of the exact geometry and similar velocity structure to the study reach were run through the velocity calculation scheme and results were compared to the original velocity field. The along-glacier and cross-glacier velocities were both reproduced to within 0.1%, although the difference in the vertical was 3.39%. The larger error in the vertical is believed to have resulted simply from truncation errors in the comparison scheme. An additional check is offered by one independent measurement of vertical velocity along a borehole [*Harper*, 1997], which matches the computed result in direction and magnitude.

Additional errors in the computed velocities were introduced in the interpolation of the 31 velocity profiles to a three-dimensional velocity field. The three-dimensional interpolation process was also tested with the synthetic data set. Of particular interest was the influence of the original data spacing on the interpolation process. Results showed that the interpolation was reliable for round 3 data, where there were 31 holes, but did not produce adequate results using the 14 holes of round 4. Therefore the three-dimensional interpolation was restricted to round 3 data.

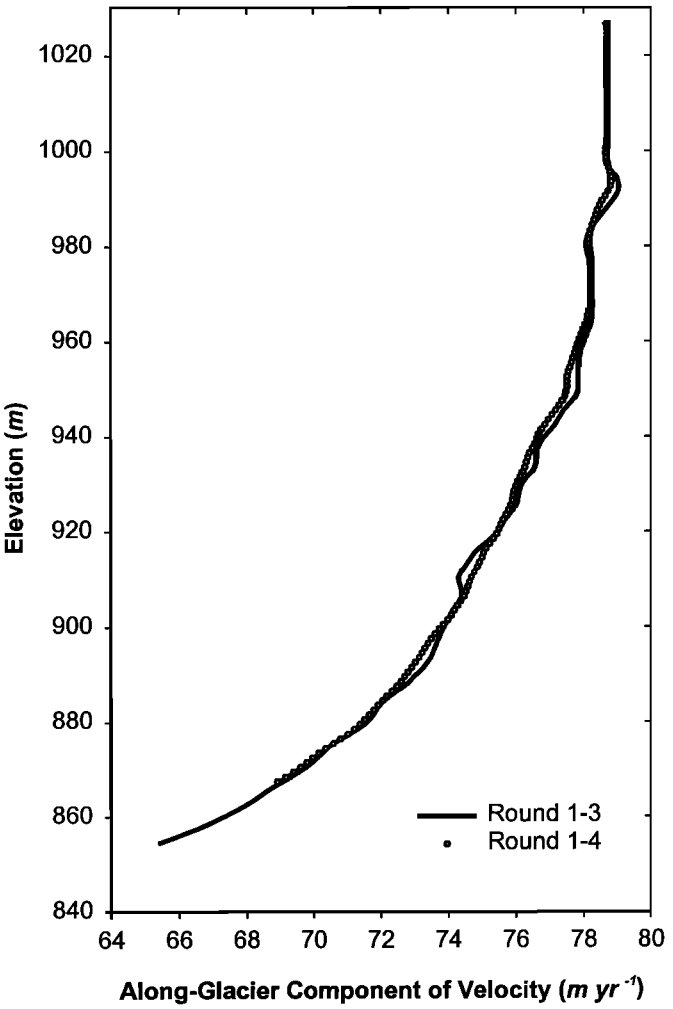

Figure 6. Comparison of round 1-3 with round 1-4 inclinometry of borehole 2WC. No evidence was found for temporal variations in the deformation of the boreholes. Local irregularities in round 1-3 profile may reflect a greater component of measurement error in the computed velocities than with round 1-4 data.

4. Results

4.1. Borehole Deformation

Internal deformation produced a relative displacement between the top of the boreholes and all points along the holes. None of the displaced hole trajectories, including those measured after approximately 30, 60, and 365 days of deformation, showed local discontinuities or signs of motion along shear planes: all borehole trajectories showed generally smooth deformation profiles from top to bottom. While diurnal, seasonal, and transient variations in surface velocity

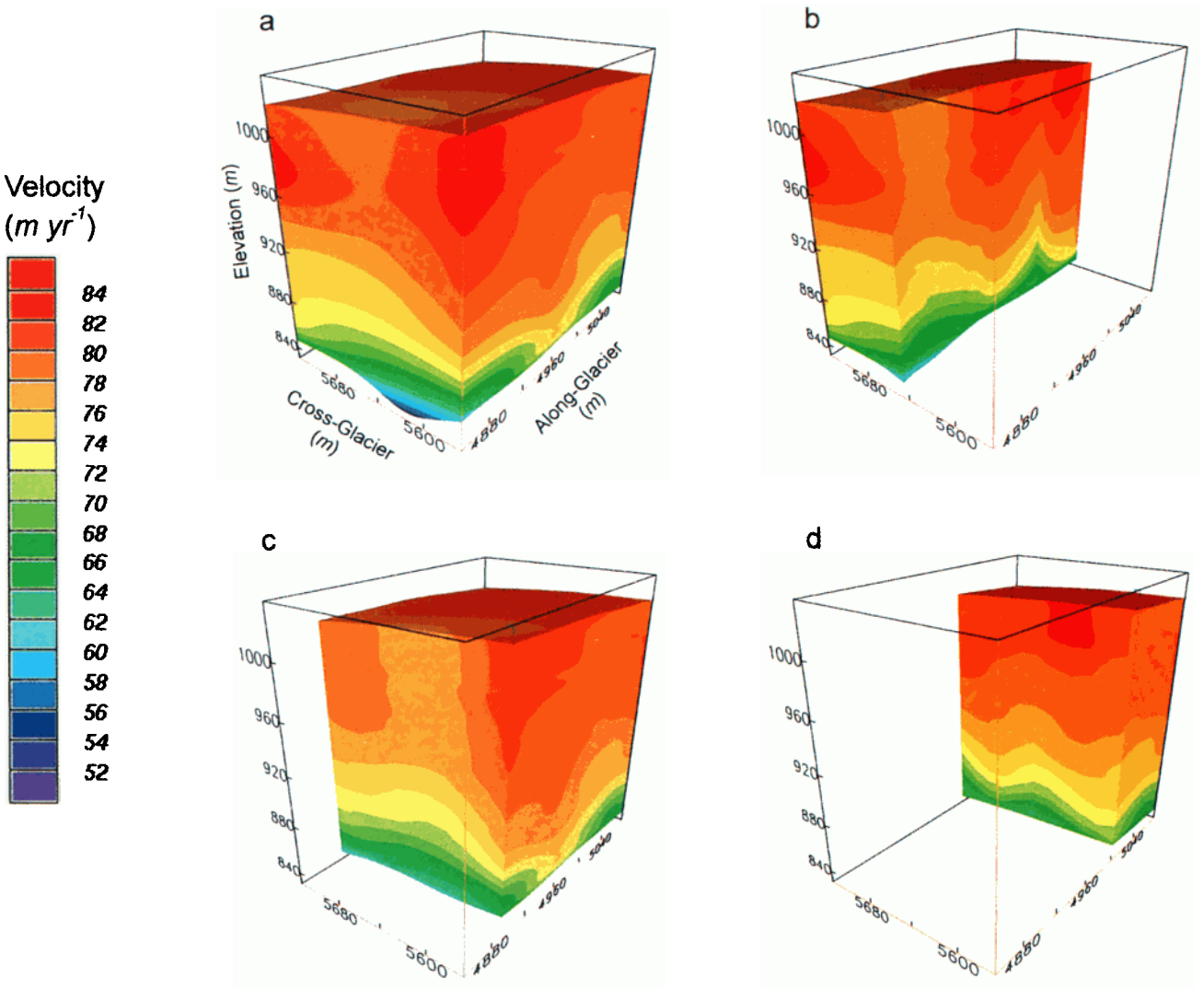

Plate 1. Perspective views of the total velocity field ($\sqrt{u_1^2 + u_2^2 + u_3^2}$) within the 6×10^6 m^3 study block. Top right and bottom panels are cut away to show structure of flow field within the block. The primary structure to the flow field is bed-parallel motion with velocity as nonlinear function of depth. Second-order features include corrugations near the bed extending along and across glacier and several anomalously fast regions at shallow depths (e.g., bottom right).

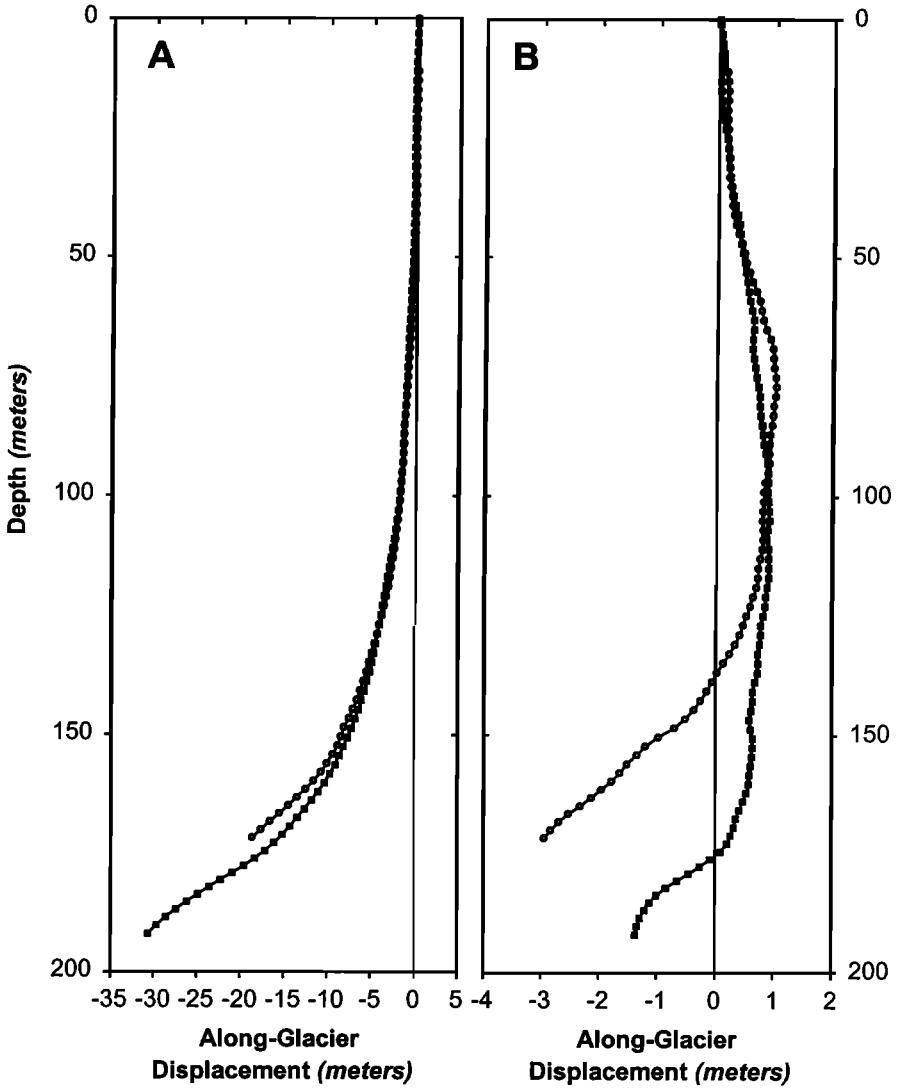

Figure 7. Profiles of two boreholes after 1 year of deformation. Plots show the displacement of points along the hole relative to the surface. (a) Along-glacier direction and (b) cross-glacier direction.

were observed [*Harper et al.*, 1996], comparison of round 3 and round 4 inclinometry profiles reveal no evidence for temporal changes in the rate of internal deformation (Figure 6). As expected, deformation was greatest in the along-glacier direction and was nearly an order of magnitude greater than in the cross-glacier direction. After a 60-70 day period the maximum displacement between the top and bottom of the holes was 3-4 m in the along-glacier direction and up to about 0.75 m in the cross-glacier direction (Figure 5). Over a 1 year period the tops of the holes were displaced of the order of 30 m in the along-glacier direction and close to 4 m in the cross-glacier direction from the bottom of the holes (Figure 7).

The year-averaged profiles have two notable differences from the short-term profiles: (1) a slight inflection point near the bed in the along-glacier direction, and (2) in the cross-glacier direction, southward directed flow from the surface to a depth of about 75 m, but northward flow below this depth. This reversal in the cross-glacier flow direction at depth was not identified in any of the 31 boreholes that were measured over the short time interval, probably because the displacements were too small over the shorter interval to be detected.

Our error analysis (section 3.4) gives an elliptical confidence region surrounding the measured hole trajectories. From this the maximum part of the displacements that could be attributable to measurement error may be determined at a particular confidence level. We are most interested in round 3 inclinometry data, since this is the most complete data set. With a confidence interval of 95% the error in these measurements is predicted to be no more than 5-10% of the observed displacements in the along-glacier direction, and up to a maximum of about 20% of the cross-glacier direction. Because of greater displacements over longer times, the error component drops for round 4 data and becomes negligible for the year-long measurements.

4.2. Velocities

The iterative scheme used to convert the borehole profiles to velocities (section 3.2) made relatively small changes to

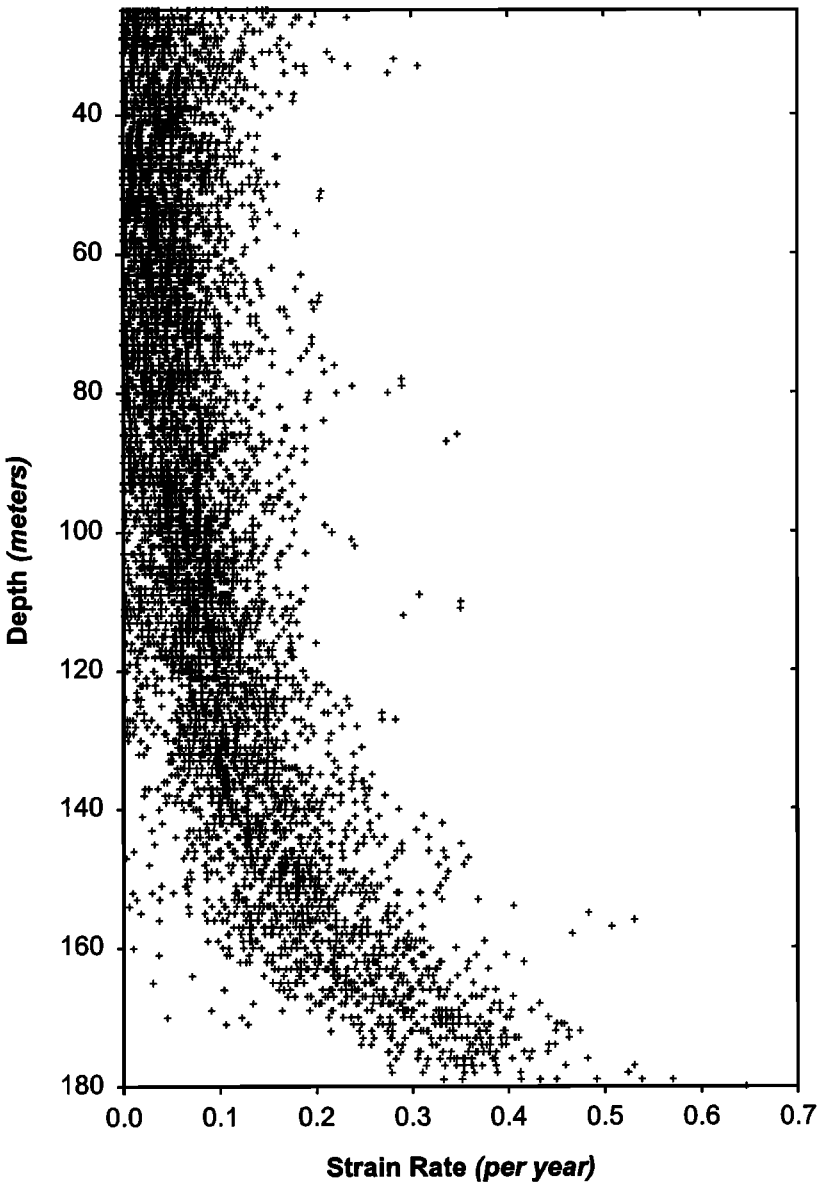

Figure 8. Computed values of strain rate at 6473 points. Strain rates were calculated by differentiation of the velocity profiles derived from deformation experiments in 31 different boreholes.

what the horizontal velocities would have been if vertical velocity had been assumed to be zero. The procedure changed velocities by about 0.5% in the along-glacier direction, while in the cross-glacier direction, the adjustment was approximately 5%. These corrections were essentially constant with depth. The calculated vertical velocities show a smooth decay from negative values at the surface to less negative values toward the bottom of the boreholes. Magnitudes of the vertical velocity at the surface ranged from near zero up to a few meters per year and show a complex and irregular spatial pattern.

The three-dimensional field of total velocity (the magnitude of the maximum velocity vector at each grid node) shows a general decrease with depth (Plate 1). Velocities near the bottom of the study block are of the order of 55-60 m yr^{-1}, while at the surface, total velocity was 75-80 m yr^{-1}. The motion is generally bed parallel and gradients in velocity were greatest within the lower 60 m of the bed [*Harper et al.*, 1998b]. Projecting the velocity field to the bed gives a sliding velocity of about 50-55 m yr^{-1}. This represents about 60-70% of the total surface velocity of the glacier.

The dominant structure of the spatial pattern of the flow field is valley-parallel flow. Nevertheless, the flow field demonstrates several more complicated elements. For example, a series of roughly 20 m long sinusoidal features are present in the lower 30-50 m of flow. These "corrugations" extend both across-glacier and along-glacier and may reflect the underlying bedrock topography, which radio-echo sounding measurements suggest has a maximum relief at a similar length scale. The corrugations are restricted to the region of high strain near the bed and do not propagate upward to the relatively undeformed surface ice. Near the surface, there are also local velocity anomalies that did not extend through the entire depth of flow. The upper 60-80 m

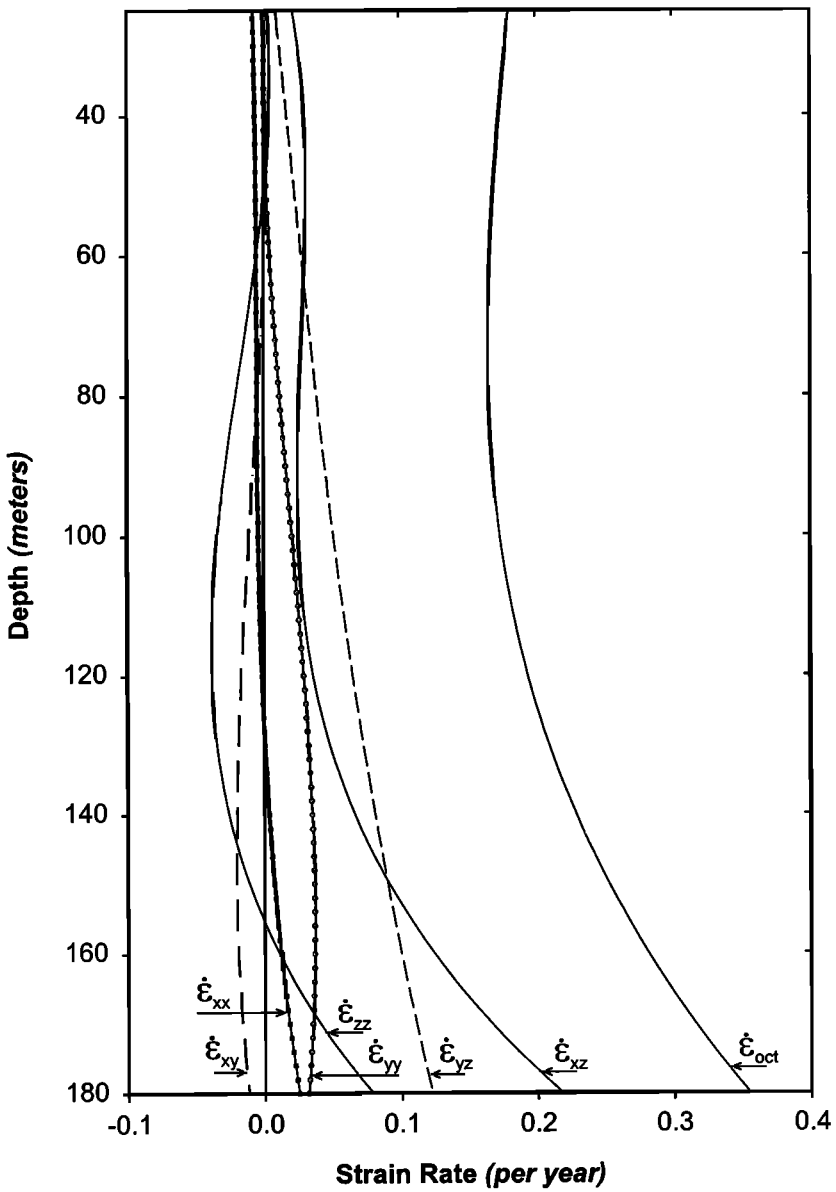

Figure 9. Average within the study block of each independent component of the second rank strain rate tensor and the octahedral strain rate. Coordinate system is defined as x, along-glacier direction; y, cross-glacier direction; z, vertical direction.

of ice along the up-glacier and down-glacier edges of the three-dimensional block move faster than the central portion (plan view) of the block. These high-velocity regions may reflect the presence of two ice falls, one just up-glacier from the reach producing compression and one just down-glacier producing tension.

4.3. Strain

The strain in the glacier is investigated through analysis of both the borehole maps and the three-dimensional velocity field; the former yield information about the pattern of strain from data in its most raw form, while the latter offers an analysis of the complete strain field. The englacial velocity profiles along individual boreholes were used to calculate strain as a function of depth. This was done by taking the velocity along the x direction as u (the deviation from the down-glacier direction is never more than a few degrees) and computing the down-glacier/vertical shear as $\partial u/\partial z$, where z is the vertical coordinate. Using a finite difference method, values of $\partial u/\partial z$ were calculated for 6473 points along velocity profiles created from round 1-3 and round 1-4 inclinometry intervals (Figure 8). The resulting data field has a wide band of scatter that may be attributed to at least several causes, including differentiation of digital data, measurement errors, and true variability in the strain rate between the different boreholes.

The general pattern of $\partial u/\partial z$ across the depth of the glacier consists of two zones: an upper zone where there is relatively little ice deformation, and a lower zone where shear strain rates are high and increase rapidly toward the bed. The upper zone has strain rates generally less than 0.15 yr^{-1}, and extends from the surface to a depth of about 120 m. In this region the strain rate shows a slight increase with depth, but the com-

puted strain rates at 100 m depth is barely distinguishable from values at 25 m depth, indicating that the upper layer of ice is essentially a uniformly deforming block. Beneath this upper zone, deformation increases rapidly toward the bed following a highly nonlinear profile. By a depth of 180 m, strain rate values are as high as about 0.4 yr^{-1}.

The components of the strain rate tensor were calculated from the three-dimensional velocity grid. Representing the three orthogonal coordinate directions (x, y, z) as (x_1, x_2, x_3) and the velocities along those directions as (u_1, u_2, u_3), the strain rate tensor $\dot{\varepsilon}_{ij}$ was computed from the spatial derivatives of the velocity field, where

$$\dot{\varepsilon}_{ij} = \frac{1}{2}\left(\frac{\partial u_i}{\partial x_j} + \frac{\partial u_j}{\partial x_i}\right) \quad (4)$$

and (i,j) are indexed from 1 to 3. The total strain, or octahedral strain rate $\dot{\varepsilon}_{oct}$, was then computed as

$$\dot{\varepsilon}_{oct} = \sqrt{\frac{\dot{\varepsilon}_{ij}\dot{\varepsilon}_{ij}}{3}} \quad (5)$$

where repeated indices are to be summed over their range.

All grid node values of each of the three-dimensional strain rate components were projected against a common depth axis and then fitted with a third-order polynomial. This reduced the components to reach-averaged curves describing the relationship between strain rate and depth. All six independent (of the nine total) components of the strain rate tensor are shown in Figure 9. The cross-glacier/vertical component of strain rate ($\dot{\varepsilon}_{yz}$) increases with depth and, despite relatively low cross-glacier velocities, is slightly greater than the along-glacier/vertical strain rate ($\dot{\varepsilon}_{xz}$). The longitudinal strain rate ($\dot{\varepsilon}_{xx}$) is an order of magnitude lower than $\dot{\varepsilon}_{xz}$, ranging from values of about -0.01 yr^{-1} at the surface to 0.02 yr^{-1} at the bed. These values represent longitudinal extension near the surface changing to longitudinal compression near the bed. The depth change is relatively linear through the upper zone but becomes more nonlinear through the lower zone. The down-glacier shear becomes significantly larger than the other terms at about two thirds of the depth of the glacier. Even at depth, $\dot{\varepsilon}_{xz}$ only makes up only about half of the octahedral strain rate, meaning that the other components accounted for as much as 50% of the total deformation. We note that our chosen orientation of the coordinate axis could be rotated. This would alter values of the individual strain rate components but not the octahedral strain rate. The three-dimensional velocity field, however, demonstrates that there is significant strain in all directions, indicating that no choice of coordinate axis could attribute all strain to along-glacier shear ($\dot{\varepsilon}_{xz}$).

5. Discussion

5.1. Three-Dimensional Measurements

Measuring the three-dimensional velocity field in temperate ice with comparable resolution in all dimensions is complicated by several difficulties. Most temperate valley glaciers are of the order of 50-500 m thick and 500-2000 m wide, and so their stress and strain fields can be expected to show structure at a length scale of tens of meters. Because basal slip accounts for as much as 60-80% of the total velocity in temperate glaciers, boreholes exhibit relatively small internal deformations as they are displaced over a distance of tens of meters. This creates difficulty in overcoming measurement errors: hundreds of meters of total displacement may be required before the borehole shows deformation at a level that can be measured well above instrument error. However, such large displacements may average the measurement over a distance that obscures important structure. This problem can be minimized by drilling initially straight and vertical holes so that errors are associated with only the final measurement of the borehole profile. In addition, since most of the measurement error is currently in the determination of azimuth, improved magnetometer design will aid in solving this problem.

In our case the horizontal velocities calculated from *Raymond*'s [1971a] iterative correction scheme are close to what they would be had the vertical velocity assumed to be zero. This is due to the fact that the horizontal velocity is nearly an order of magnitude greater than the vertical velocity and the glacier thickness was relatively constant over the displacement paths of the boreholes. However, while not necessary for computing the horizontal velocities in this situation, the scheme has the benefit of yielding vertical velocities.

Calculation of the three-dimensional velocity field from measurements of borehole deformation requires that borehole coordinates be tracked in three-dimensional space. This is done by measuring the offset between points along the hole and the hole collar at the glacier surface. Consequently, accurate surveying of the borehole collar is especially critical as "hanging" the borehole from a mislocated point at the surface will cause significant velocity errors throughout the depth of flow.

5.2. Spatial Variability

Worthington Glacier has a relatively simple geometry in the vicinity of the study reach. The valley walls are approximately parallel, there are no ice tributaries, and the surface slope is low and nearly uniform. Thus there are no major features within the reach that would complicate the stress field. There should be three major categories of stresses within the reach: (1) along-glacier shear, increasing uniformly with depth; (2) locally produced stresses related to minor variations in the bed, surface slope, and valley walls; (3) stresses related to far-field glacier dynamics that are transferred over lengths equivalent to multiple ice thicknesses. The three-dimensional data collected on Worthington Glacier should give an indication of the relative importance of each of these sources of stress in determining the state of flow within this valley glacier.

The simple "slab on a slope" model for glacier flow [e.g., *Paterson*, 1994] assumes that deformation is driven by shear in the vertical/along-glacier plane (τ_{xz}). The deformation near the surface is assumed to be zero as τ_{xz} falls below the yield stress of ice. Worthington Glacier's octahedral strain rate is essentially constant in the upper two thirds of the ice thickness. However, there is significant deformation in this zone resulting from small strain rates in all directions. Thus, while small longitudinal and transverse stresses do not produce large surface velocities, their combined effect serves to deform the ice more than is expected from plane strain in the vertical/along-glacier direction. The shear-strain rate component $\dot{\varepsilon}_{xz}$ does not dominate the total deformation profile until a depth of about 120 m. From here to the bed, how-

ever, the deformation increases rapidly on a nonlinear profile, presumably driven by much higher shear stress in the x-z plane.

The three-dimensional deformational pattern of flow has several complicating features. Anomalously fast areas are located along the up-glacier and down-glacier edges of block. These are likely the result of longitudinal stresses induced by Worthington Glacier's two large icefalls. The edges of the study reach are approximately 200 m below one icefall and 300 m above another. If the high-velocity zones are indeed related to the icefalls, this implies that the icefalls influence the flow field over a length scale that extends of the order of 1 to 2 ice thicknesses along the length of the glacier. Additional complexity in the flow field is present in the form of "corrugations" in the flow field near the bed. These could be related to variations in sliding rate and/or variations in the deformation field caused by subglacial topography. *Balise and Raymond* [1985] and *Bahr et al.* [1994] predict through modeling work that basal disturbances of less than five ice thicknesses will not be observable at the surface. The three-dimensional flow field shows that such disturbances are indeed present, and confirms that they are not propagated to the surface velocity field. Finally, the flow field displays a reversal in the cross-glacier flow direction at depth. The cause of this flow reversal is uncertain, but its presence is further indication that the ice within the reach is deforming in response to more than simple shear.

The above observations demonstrate that the flow of Worthington Glacier deviates considerably from classic laminar flow, where particle paths are everywhere parallel to each other and to the bed. However, the deviations are all second-order effects; they represent deformation rates that are nearly an order of magnitude smaller than the along-glacier shear strain. Nevertheless, short-wavelength variations in velocity of the order of 5-10 m yr^{-1} cannot be considered insignificant.

6. Conclusions

This work demonstrates that the full three-dimensional flow field in temperate ice may be measured from borehole inclinometry of an array of uncased boreholes. Because the primary mechanism of motion is basal slip, small magnitudes of internal deformation must be resolvable in order to capture the flow field with similar resolution in all dimensions. Boreholes that display significant deformation will have been displaced so far through the flow field that they represent a spatial average of flow. This presents a paradox: small displacements are required for accurate measurement of the three-dimensional flow field, but small displacements will have a relatively greater proportion of instrument error and thus will yield a less accurate result. This problem was surmounted by measuring the deformation of boreholes after they had been displaced a distance equivalent to approximately 5% of the ice thickness. This produced horizontal offsets between the top and bottom points along the holes of 3-4 m along the glacier and 0.75 m across the glacier. Random and instrumental errors were then documented by pooling error information from measurements in 31 different boreholes.

The spatial pattern of flow in a 6×10^6 m^3 study block of Worthington Glacier shows generally bed-parallel flow. Motion is dominated by basal slip with only 30-40% of velocity due to internal deformation. The pattern of deformation varies in the vertical dimension to form two general regions: an upper zone of relatively constant strain rate that extends from the surface to a depth of about 120 m, and a lower zone of high and non-linearly increasing strain rate that extends from 120 m to the bed. Close to the bed the octahedral strain rate is 0.35 m yr^{-1} and is dominated by shear in the along-glacier/vertical plane. However, deformation rates in the upper zone are nearly half this amount due to small strains in all directions.

The three-dimensional velocity field shows structure at a length scale of the order of tens of meters, both near the surface and the bed. None of the velocity features extends through the entire depth of flow but are limited to either the upper constant strain rate region or the lower highly deforming region. Locally, fast moving areas present near the surface are likely caused by longitudinal forcing from icefalls located above and below the study reach. Near the bed, roughly 20 m long corrugations in the velocity field extend along and across glacier, probably reflecting subglacial topography. A reversal in the cross-glacier flow direction at depth has an unknown origin. No motion along ductile zones or shear planes within the ice mass nor any time-varying deformation rates were observed.

The valley and bed geometry near the study reach on Worthington Glacier is relatively simple and uniform. Yet the flow field in this region demonstrates intricate structure at a short length scale, only some of which we can explain. This implies that the three-dimensional flow field of most valley glaciers is spatially complex, showing large departures from simple plane strain at length scales significantly smaller than the ice thickness.

Acknowledgments. Funded by grants from the National Science Foundation (OPP-9122966 to Neil F. Humphrey and OPP-9122916 to W. Tad Pfeffer). This work has benefitted from the contributions of many, including, M. Meier, B. Raup, M. Greenwood, C. Stevens, L. Bradley, D. Bradley, Alaska Department of Transportation, and Alaska State Parks. This manuscript was greatly improved by detailed comments from E. Waddington and an anonymous reviewer.

References

Alley, R. B., D. E Lawson, E. B. Evenson, J. C. Strasser, and G. Larson, Glaciohydraulic supercooling: A freeze-on mechanism to create stratified, debris-rich basal ice, II, Theory, *J. Glaciol.*, *44*, 563-569, 1999.

Bahr, D. B., W. T. Pfeffer, and M. F. Meier, Theoretical limitations to englacial velocity calculations, *J. Glaciol.*, *40*, 509-518, 1994.

Balise, M. J., and C. F. Raymond, Transfer of basal sliding variations to the surface of a linearly viscous glacier, *J. Glaciol.*, *31*, 308-318, 1985.

Blake, E. W., and G. K. C. Clarke, Interpretation of borehole-inclinometer data: A general theory applied to a new instrument, *J. Glaciol.*, *38*, 113-124, 1992.

Brecher, H. M., Surface velocity variations on the Kashawulsh Glacier, in *Icefield Ranges Research Projects: Scientific Results*, vol. 1, edited by V. C. Bushnell and R. H. Ragle, pp. 127-144, Am. Geogr. Soc. and Arctic Inst. of North America, Calgary, Alta., 1969.

Briggs, I. C., Machine contouring using minimum curvature, *Geophysics*, *39*, 39-48, 1974.

Brzozowski, J. and R. LeB. Hooke, Seasonal variations in surface velocity of the lower part of Stroglaciären, Kebnekaise, Sweden, *Geogr. Ann.*, *63A*, 233-240, 1981.

Echelmeyer, K. A., W. D. Harrison, C. F. Larsen, J. Sapiano, J. E. Mitchell, J. DeMallie, B. Rabus, G. Adalgeirsdóttir, and L.

Sombardier, Airborne surface profiling of glaciers: A case-study in Alaska, *J. Glaciol.*, *42*, 538-547, 1996.

Engelhardt, H., N. Humphrey, B. Kamb, and M. Fahnestock, Physical conditions at the base of a fast moving Antarctic ice stream, *Science*, *248*, 57-59, 1990.

Harbor, J., M. Sharp, L. Copland, B. Hubbard, P. Nienow, and D. Mair, Influence of subglacial drainage conditions on the velocity distribution within a glacier cross section, *Geology*, *25*, 739-742, 1997.

Harper, J. T., The three-dimensional flow field of a temperate ice mass: Surface and borehole deformation studies on Worthington Glacier, Alaska, Ph.D. dissertation, Univ. of Wyo., Laramie, 1997.

Harper, J. T., and N. F. Humphrey, Borehole video analysis of a temperate glacier's englacial and subglacial structure: Implications for glacier flow models, *Geology*, *23*, 901-904, 1995.

Harper, J. T., N. F. Humphrey, W. T. Pfeffer, and B. C. Welch, Short wavelength variations in the horizontal velocity field of a valley glacier, in *Glaciers, Ice Sheets and Volcanoes: A Tribute to Mark F. Meier, Spec. Rep. 96-27,* edited by S. C. Colbeck, pp. 41-48, U.S. Army Cold Reg. Res. and Eng. Lab., Hanover, N.H., 1996.

Harper, J. T., N. F. Humphrey, and W. T. Pfeffer, Crevasse patterns and the strain-rate tensor: A high resolution comparison, *J. Glaciol.*, *44*, 68-76, 1998a.

Harper, J. T., N. F. Humphrey, and W. T. Pfeffer, Three-dimensional deformation measured in an Alaskan glacier, *Science*, *281*, 1340-1342, 1998b.

Harrison, W. D., Temperature of a temperate glacier, *J. Glaciol.*, *11*, 15-29, 1972.

Harrison, W. D., A measurement of surface-perpendicular strain-rate in a glacier, *J. Glaciol.*, *14*, 31-37, 1975.

Harrison, W. D., C. F. Raymond, and P. MacKeith, Short period motion events on Variegated Glacier as observed by automatic photography and seismic methods, *Ann. Glaciol.*, *8*, 82-89, 1986.

Hooke, R. LeB., P. Holmlund, and N. R. Iverson, Extrusion flow demonstrated by borehole deformation measurements over a riegel, Storglaciären, Sweden, *J. Glaciol.*, *33*, 72-78, 1987.

Hooke, R. LeB., V. A. Pohjola, P. Jansson, and J. Kohler, Intra-seasonal changes in deformation profiles revealed by borehole studies, Storglaciären, Sweden, *J. Glaciol.*, *38*, 348-358, 1992.

Humphrey, N., and K. Echelmeyer, Hot-water drilling and borehole closure in cold ice, *J. Glaciol.*, *36*, 287-298, 1990.

Iken, A., and R. Bindschadler, Combined measurements of subglacial water pressure and surface velocity of Findelengletscher, Switzerland: Conclusions about drainage system and sliding mechanism, *J. Glaciol.*, *32*, 101-119, 1986.

Jacobel, R., Short-term variations in velocity of South Cascade Glacier, Washington, USA, *J. Glaciol.*, *28*, 325-332, 1982.

Johnson, R. A., and D. W. Wichern, *Applied Multivariate Statistical Analysis*, 2nd ed., Prentice-Hall, Englewood Cliffs, N. J., 1988.

Krimmel, R. M., and B. H. Vaughn, Columbia Glacier, Alaska: Changes in velocity, 1977-1986, *J. Geophys. Res.*, *92*, 8961-8968, 1987.

Meier, M. F., Mode of flow of Saskatchewan Glacier, Alberta, Canada, *U.S. Geol. Surv. Prof, Pap. 351*, 70 pp., 1960.

Meier, M., S. Lundstrom, D. Stone, B. Kamb, H. Engelhardt, N. Humphrey, W. W. Dunlop, M. Fahnestock, R. M. Krimmel, and R. Walters, Mechanical and hydrologic basis for the rapid motion of a large tidewater glacier, 1, Observations, *J. Geophys. Res.*, *99*, 15,219-15,229, 1994.

Paterson, W. S. B., Vertical strain-rate measurements in an Arctic ice cap and deductions from them, *J. Glaciol.*, *17*, 3-12, 1976.

Paterson, W. S. B., *The Physics of Glaciers*, 3rd ed., Pergamon, New York, 1994.

Pfeffer, W. T., N. F. Humphrey, J. T. Harper, B. Krob, and B. Amadei, In situ stress measurements in temperate ice (abstract), *Eos Trans. AGU*, *79*(45), Fall Meet. Suppl., F247, 1998.

Pfeffer, W. T., N. F. Humphrey, B. Amadei, J. T. Harper, and J. Wegmann, In situ stress tensor measured in an Alaskan glacier, *Ann. Glaciol.*, *31*, 229-235, 2000.

Raymond, C. F., Determination of the three-dimensional velocity field in a glacier, *J. Glaciol.*, *10*, 39-53, 1971a.

Raymond, C. F., Flow in a transverse section of Athabasca Glacier, Alberta, Canada, *J. Glaciol.*, *10*, 55-84, 1971b.

Sapiano, J. J., W. D. Harrison, and K. A. Echelmeyer, Elevation, volume and terminus changes in nine glaciers in North America, *J. Glaciol.*, *44*, 119-135, 1998.

Shreve, R. L., and R. P. Sharp, Internal deformation and thermal anomalies in lower Blue Glacier, Mount Olympus, Washington, U.S.A., *J. Glaciol.*, *9*, 65-86, 1970.

Stone, D. B., M. F. Meier, K. J. Lewis, and J. T. Harper, Drainage configuration and scales of variability in the subglacial water system (abstract), *Eos Trans. AGU*, Fall Meet. Suppl., *75*(44), 222, 1994.

Taylor, P. L., A hot water drill for temperate ice, *CRREL Spec. Rep. 84-34*, pp. 105-117, Cold Reg. and Eng. Lab., Hanover, N. H., 1984.

Welch, B. C., W. T. Pfeffer, J. T. Harper, and N. F. Humphrey, Mapping subglacial surfaces below temperate valley glaciers using 3-dimensional radio-echo sounding techniques, *J. Glaciol.*, *44*, 164-170, 1998.

D. B. Bahr, J. T. Harper, and W. T. Pfeffer, Institute of Arctic and Alpine Research, University of Colorado, Boulder, CO 81309. (David.bahr@colorado.edu; joelh@tintin.colorado.edu; pfeffer@tintin.colorado.edu)

N. F. Humphrey and B. C. Welch, Department of Geology and Geophysics, University of Wyoming, Laramie, WY 82071. (Neil@uwyo.edu; welchb@uwyo.edu)

S. Huzurbazar, Department of Statistics, University of Wyoming, Laramie, WY 82071. (lata@uwyo.edu)

(Received August 19, 1999; revised September 1, 2000; accepted November 28, 2000.)